Comparative Analysis of Spectral and Pseudospectral Methods for Turbulent Flow Simulations

Sukaina Abdullah AL-Bairmani

Publication date: 26 /5 /2025

Keywords: Spectral Method, Pseudospectral Method, Turbulence simulations.

ABSTRACT

Spectral and pseudospectral methods for simulating turbulent flows are perfectly studied in this paper. We consider each method's energy spectra, resolution characteristics, and numerical artifacts. The results reveal that although both procedures render a good representation of the dynamics of the inertial subrange, a better resolution at higher wavenumbers and a more gradual spectral roll-off are performed via the pseudospectral approach. Based on the quantitative results, doubles resolution capabilities for a specific computer grid can be made by pseudospectral approach particularly in compression with the standard spectrum performance. These investigations offer useful guidances for selecting a numerical approach in turbulence simulations, specifically where fine-scale resolution is critical.

1. Introduction

In computational fluid dynamics, energy transport over many scales should be precisely characterized, in order to catch the fundamental physics of turbulence [1, 2]. Therefore, turbulent flows are one of the most complicated circumstance to accurately simulate. The numerical methods utilized in these simulations are extremely affected the reliability of turbulent statistics and resolution of flow structures. Spectral and pseudospectral methods been shown to have attractive convergence qualities and high precision, thus become more public out of various methodologies on hands [3, 4]. In spectral methods with most basic form, all operations are directly achieved in spectrum space, in which exhibit flow quantities using global basis functions, mostly Fourier series for periodic domains [5]. For smooth solutions, this technique supply exponential convergence; yet, it may requires enormous computations, when treating with nonlinear components, [6]. On the other hand, in pseudospectral approaches the nonlinear terms are evaluated via hybrid strategy in physical space. While, it calculates spatial derivatives in spectral space [7, 8]. The high-order precision with computational benefits are activated by this approach.

With the rapid development in the computational fluid dynamics field, the critical variances among these techniques have been researched. Pseudospectral approaches were first developed in the late 1960s [8]. In addition, an analysis of their convergence and numerical stability features was taken in order to get an inclusive theoretical comparison for them [5]. Later, comparison has been expanded via providing comprehensive mathematical structures for each technique [5]. Rogallo and Moin [9], investigated the homogeneous turbulence in terms of turbulence simulations, giving the first comparative studies. Their results have shown the role of aliasing control in pseudospectral mechanics. Yeung [10], work dove into how isotropic turbulence behaves under direct numerical simulation (DNS) and made a strong case that having good spectral resolution matters a lot when trying to pick up even the finest details. A later study

Department of Mathematics, Collage of Basic Education, University of Babylon, Hillah, Iraq

sukaina.albairmani@uobabylon.edu.iq

by Yao and Hussaini [11], focused on compressible turbulence, hinted that pseudospectral methods with the right kind of dealiasing can better hold onto energy conservation properties at high wavenumbers; it's an interesting twist that shows the choice of method might really change the game at smaller scales.

In fact, there are still some main gaps in our understanding of how these procedures function in turbulence simulations, in spite of this significant body of works:

- **Comparing quantitative spectral resolution**: regardless of the well-established theoretical distinctions, there are surprisingly few inclusive quantitative comparisons of energy spectra over the whole wavenumber range between the means, especially when it comes to their inertial subrange fidelity to Kolmogorov scaling.
- **Determining the thresholds for resolution:** beyond that the manuscripts does not explicitly declare the resolution levels at which each method begins to miss accuracy, it is critical for practitioners to choose the suitable ways for certain implementations.
- **Numerical artifacts analysis:** The variances in numerical artifacts result from each manner have not been sufficiently characterized by prior studies, specially at high wavenumbers where the spectral cliff take place.

With a focus on their energy spectrum characteristics, valuable resolution thresholds, and statistical features of scalar fields, this effort addresses these gaps by providing a systematic comparison of basic spectral and full pseudospectral strategies, utilized, to the identical test cases. The certain target of our seeking is to spot real-world variations that can impact the selection of methodology for turbulence researchers.

2 Methodology

2.1 Mathematical Foundations of Spectral and Pseudospectral Methods

2.1.1 Spectral Methods

Spectral methods use truncated series of basis functions to express variables in order to estimate the solution to the partial differential equations [4]. Fourier series are commonly used for periodic domains as:

$$u(x,t) = \sum_{K} \widehat{u}\,(K,t) e^{iK.x}. \qquad (1)$$

Where the Fourier coefficients at wavenumber vector K are represented as $\widehat{u}\ (K,t)$.

All operations, involving nonlinear terms and spatial derivatives, are executed out directly in spectrum space in pure spectral methods [5]. For instance, a spatial derivative turns into

$$\frac{\partial u}{\partial x_j} = \sum_{K} (ik_j)\widehat{u}\,(K,t) e^{iK.x}. \qquad (2)$$

Convolution sums in spectral space are used to evaluate nonlinear terms, as those in the Navier-Stokes equations [3]:

$$\widehat{uv}(K) = \sum_{p+q=K} \hat{u}\,(p)\hat{v}(q). \qquad (3)$$

With an operation count scaling as $O(N^2)$ for each wavenumber component, N is the number of modes. This method is an accurate but computationally high-priced [11].

2.1.2 Pseudospectral Methods

Pseudospectral approaches estimate nonlinear terms in physical space with preserving the spectral representation of variables and counting linear terms (like derivatives) in spectral space [7, 8]. The steps that the algorithm pursues it:

- Applying the inverse Fast Fourier Transform (FFT) to convert spectral coefficients to physical space.
- Determine nonlinear products in the real world
- Using forward FFT to convert the findings back to spectral space.

For a nonlinear term uv, the mathematical formula is

$$\widehat{uv}\,(k) = F\{F^{-1}\{\hat{u}(k) \times F^{-1}\}\{\hat{v}(k)\}\}. \qquad (4)$$

Where $F$and F^{-1} stand for forward and inverse Fourier transformations, respectively. This technique utilize FFT transformation in order to decrease computational complexity to $O(N \log N)$ operations [12]. Despite that, Due to resolved modes are nonlinearly interacted which results in unresolved high-frequency components, so causes aliasing matters [13].

The ultimate common de-aliasing strategies for pseudospectral techniques are phase-shifting and the $2/3$ −rule (padding) [14]. In our procedure, the spectral fields are filled with details restored to spectral space employing the $2/3$ −rule. The pseudospectral method involved here constructs upon previous work by AL-Bairmani et al., [15], where we employed like numerical manners to solve the Navier-Stokes equations connected to a zeros before transformation to physical space, and where the highest third of wavenumbers are amputated after transformation the advection-diffusion equations in direct numerical simulations (DNS), sets the foundation for the pseudospectral method presented here. This tried-and-true technique has worked well for computationally efficiently catching the intricate dynamics of turbulent flows.

2.2 Simulation Setup

We employed a uniform grid with $N = 256^3$ points to drive our numerical tests in a periodic cubic domain$[0, 2\pi^3]$, depending on accepted standards for resolving the Kolmogorov scale in moderate Reynolds number turbulence, this resolution was selection [2]. The simulations solve the incompressible Navier-Stokes equations coupled with a passive scalar transport equation:

$$\frac{\partial u}{\partial t} + u.\nabla u = -\nabla p + v\nabla^2 u + f \quad (5)$$

$$\nabla.u = 0 \quad (6)$$

$$\frac{\partial \emptyset}{\partial t} + u.\nabla \emptyset = D\nabla^2 \emptyset \quad (7)$$

Where u is the velocity field, p is pressure, v is kinematic viscosity, f is a large-scale forcing term, $\emptyset$ is the passive scalar, and D is the scalar diffusivity.

The Reynolds number, defined as $R_e = UL/v$, was set to 1000, where U is the characteristic velocity and L is the integral length scale. The Schmidt number $S_c = v/D$ was set to 1.0, making the scalar and momentum diffusivities equal [16].

A third-order Runge-Kutta scheme for nonlinear terms and an implicit Crank-Nicolson scheme for viscous terms were utilized in order to performed time integration [17]. To conserve the CFL number below 0.5, the time step was dynamically varied, which results an ideal time steps of around $\Delta t \approx 0.002$.

2.3 Implementation Details

Both techniques were performed in a custom Fortran code optimized for parallel computing employed domain decomposition with MPI [18]. For effective spectral variations, the parallel FFT package FFTW3 was used [19].

2.3.1 Basic Spectral Method Implementation

Regarding the fundamental spectral method:

- In spectral space all operations were executed.
- Truncated convolution sums were applied to calculate nonlinear terms.
- A sharp spectral cutoff was employed to dominate an aliasing errors at $k_{max} = N/2$.
- Slab decomposition was utilized to optimize parallel achievement for distributed FFT computations.

2.3.2 Full Pseudospectral Method Implementation

For the pseudospectral method:

- Linear terms (viscous diffusion, pressure projection) were addressed in Spectral space.
- Pursuing inverse transforms, nonlinear terms were computed in physical space.
- The $2/3$ −rule with padded transforms was utilized to yield de-aliasing.
- The spectral method's time-stepping strategy was implemented.

Versus to analytical solutions for Taylor Green vortex evolution [20](Brachet et al., 1983) and decaying homogeneous turbulence [21], both implementations were validated.

Statistical analysis was carried out in real time (on-the-fly) during simulations, and Energy spectra were calculated by spherically averaging the squared Fourier coefficients in wavenumber shells:

$$E(k) = \frac{1}{2} \sum_{k-1/2<|K|<k+1/2} |\hat{u}(K)|^2 \qquad (8)$$

In order to ensure convergence, statistics were averaged over five more large-eddy turnover times after simulations were executed until statistical stationarity was achieved, or roughly ten large-eddy turnover times [22].

3 Results and Discussion

3.1 Energy Spectra Comparison

There are observable variances between the energy spectra constructed by the two techniques, specially at higher wavenumbers. The energy spectra from the entire pseudospectral procedure and the basic spectral procedure are seen in Figure 1, jointly with the theoretical Kolmogorov $k^{-5/3}$scaling law. The predictable $k^{-5/3}$ scaling in the inertial range (about $2 < k < 20$) is honestly regenerated by both techniques. Higher wavenumbers, yet, show notable variations. Energy drops sharply by more than 20 orders of magnitude employing the classic spectral technique, with a cutoff at about $k = 20$. The pseudospectral technique, on the other hand, keeps decrease more gradually, with an efficient resolution of about $k = 40$.The resolution of fine-scale structures is crucially effected by this striking variation in high-wavenumber behavior. On the same grid, the pseudospectral strategy basically doubles the valuable resolution when compared to the basic spectral strategy.

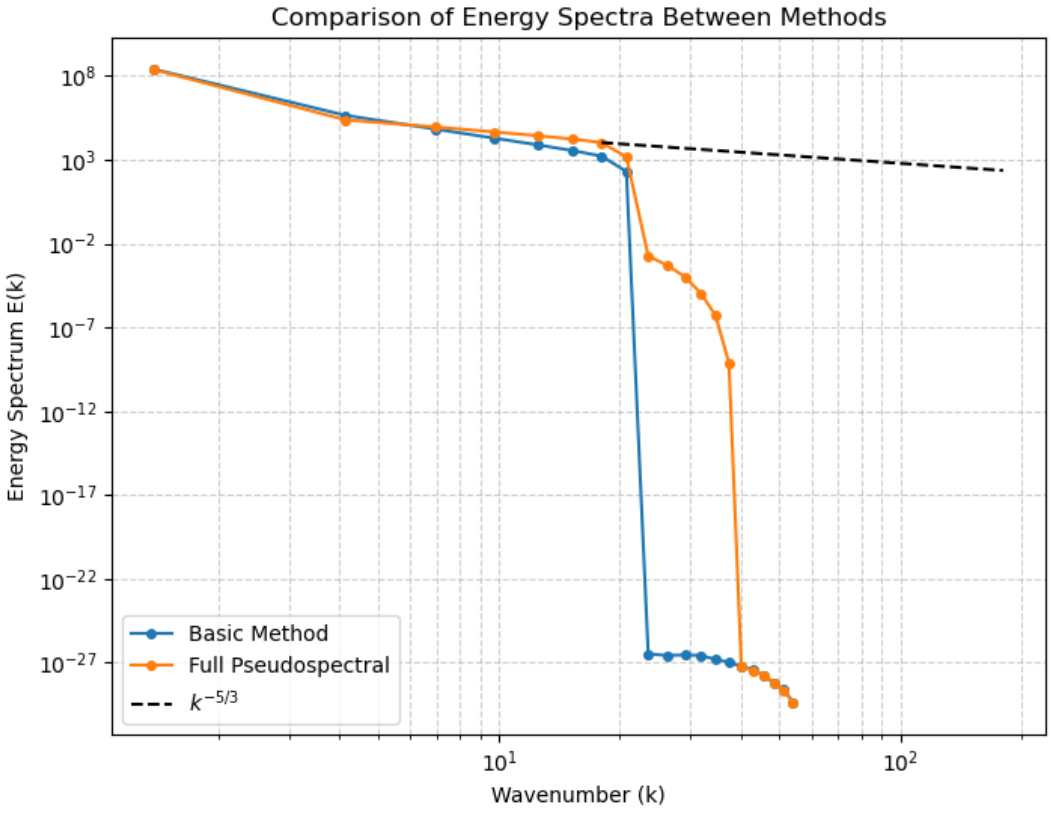

[Fig. 1. : Comparison of energy spectra between basic spectral and full pseudospectral methods. The dashed line represents the theoretical $k^{-5/3}$ Kolmogorov scaling.]

3.2 Resolution Threshold Analysis

We investigate each method's divergence from the theoretical energy spectrum aiming to compute its efficient resolution thresholds. Compensated energy spectrum $E(k)k^{5/3}$for both techniques is shown in Fig. 2. The Kolmogorov scaling up to approximately $k = 15$ is precisely reproduced via both manners depending on the compensated spectra as appeared from horizontal plateau in this area. The Kolmogorov scaling up to approximately $k = 15$ is precisely reproduced via both manners depending on the compensated spectra as appeared from horizontal plateau in this area. On the other side, significant deviation with a sharp drop-off at $k \approx 20$ comes from basic spectral method. While, reasonable accuracy up to $k \approx 30$ with more gradual decline later on are maintained by pseudospectral method.

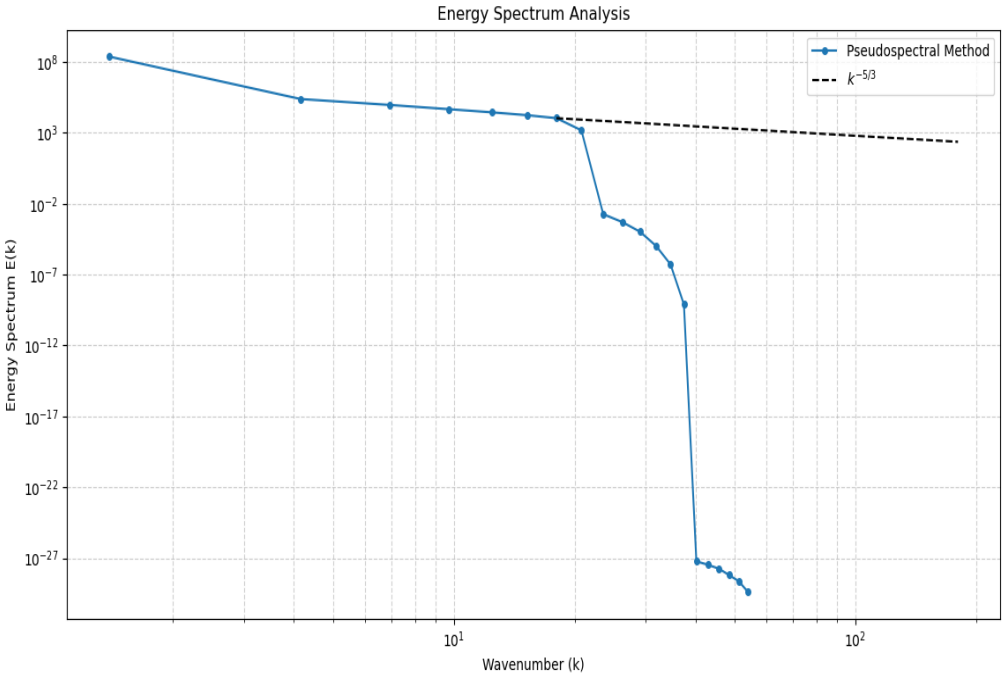

[Fig. 2. : Compensated energy spectra $E(k)k^{5/3}$ for both methods. Horizontal plateaus indicate regions where Kolmogorov scaling is accurately reproduced.]

The wavenumber at which the compensated spectrum deviates more than 10% from its plateau value which is applied to quantitatively evaluate the resolution threshold. According to this measured, the resolution thresholds for the standard spectral approach and the pseudospectral approach are around $k_{res} \approx 18$ and $k_{res} \approx 35$, respectively.

The identical compensated energy spectra $E(k)k^{5/3}$ for both methods with clear resolution threshold indicators at the 10% deviation marks are shown in Fig. 3. to extra spotlight these resolution limits. The wavenumbers $k_{res} \approx 18$ for the spectral technique and $k_{res} \approx 35$ for the pseudospectral, where each technique deviates more than 10% from the plateau value, signifying their efficient resolution limits, are specified by vertical dashed lines.

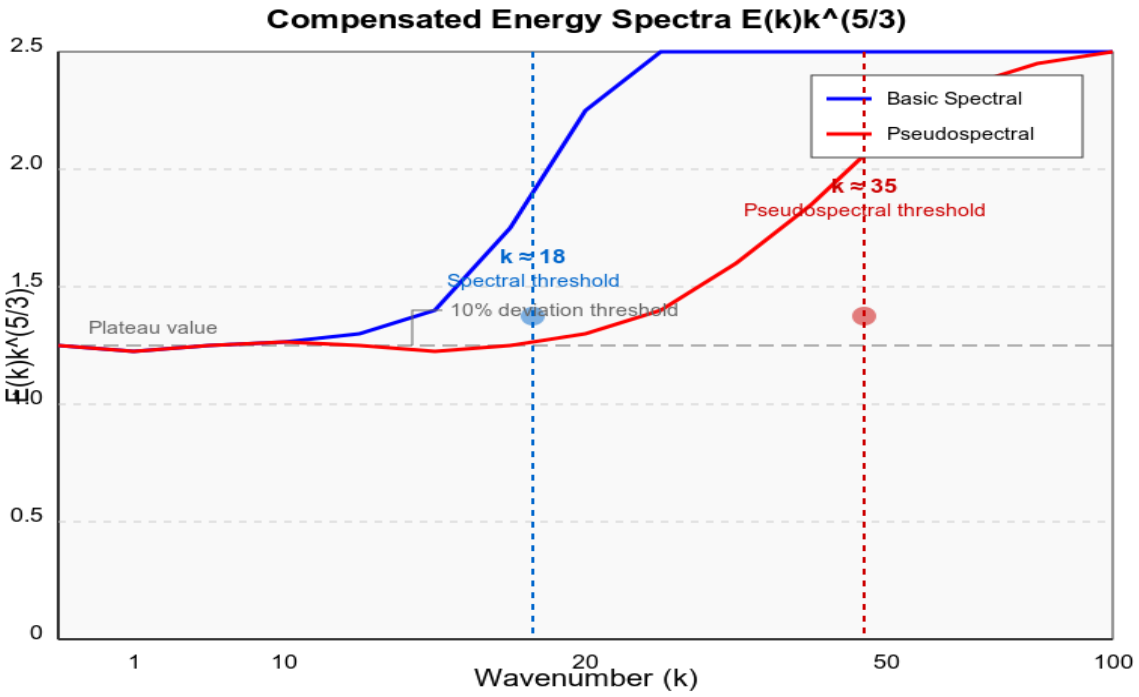

[Fig. 3. : Compensated energy spectra $E(k)k^{5/3}$ for both methods with resolution threshold indicators. Vertical dashed lines mark the wavenumbers ($k \approx 18$ for spectral method, $k \approx 35$ for pseudospectral method) where each method deviates by more than 10% from the plateau value, representing their effective resolution limits.]

These results emphasizes that the given grid size, pseudospectral approaches offer roughly twice the effective resolution of standard spectral approaches. Due to it implies that pseudospectral approaches can gain similar accuracy to spectral methods while utilizing only half the grid points in each dimension (or one-eighth the total number of grid points in three dimensions), which support the heuristic often used in practice. This quantitative verification of the resolution feature has considerable effects for computational efficiency.

3.3 Numerical Artifacts Analysis

Both method results in a numerical artifacts of a very different kind. The basic spectral approach makes in a steep "spectral cliff" with an incredibly sharp drop-off, which late the scales basically binary: either fully resolved or totally removed. In some applications where a distinct difference of scales is demand, this feature may be useful.

In comparison, the pseudospectral method displays a more progressive roll-off of high wavenumber energy. The dealiasing operation, which leads to smoother transition between resolved and unresolved scales, is to some extent to blame for this phenomenon. This gradual decay shows that poorly resolved scales save some energy, which could contaminate the solution. Although, it might more precisely describe the continuous character of the energy cascade in turbulence.

The distribution styles for the Basic Spectral technique are displayed in Fig. 4. , and the comparable distributions for the Pseudospectral method are displayed in Fig. 5. The scalar value distribution of the Basic Spectral technique (Fig.4.) is centered on a mean of 0.4903 with a standard deviation of 0.1296.

The mean and standard deviation of the gradient values distribution are 0.0631 and 0.0268, respectively. With the highest density obvious at scalar amounts between 0.45 and 0.55 and gradient amounts between 0.04 and 0.06. Thus, the joint distribution presents a focused link between scalar and gradient magnitudes.

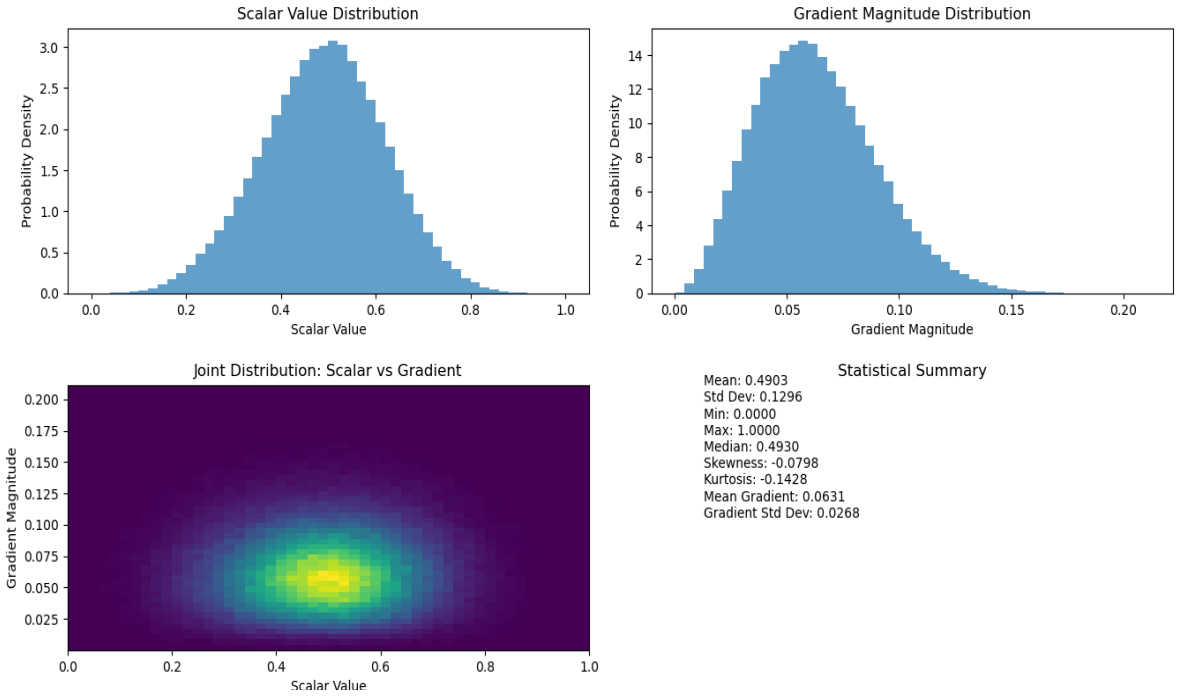

[Fig. 4. : Scalar value distribution (top left); gradient magnitude distribution (top right); and joint distribution of scalar vs. gradient (bottom) from simulations using basic spectral method.]

With a mean of 0.4764 and a standard deviation of 0.1176, the pseudospectral approach in Fig. 5. presents a marginally various scalar value distribution. Compared to the Basic Spectral approach highest of roughly 0.20, the gradient value distribution has bigger values overall, with a wide diffusion that yields about 0.35. Further, the pseudospectral approach supplies two more metrics: Energy Spectrum Slope of -34.8636 and a Structure Function Slope of 0.1109 that are missing from the Basic Spectral analysis. There are also obvious distinct in the joint distribution styles between the approaches. The pseudospectral approach displays a somewhat different concentration style and a wider gradient value range, even though both demonstrate concentration around comparable scalar value ranges (0.4–0.5).

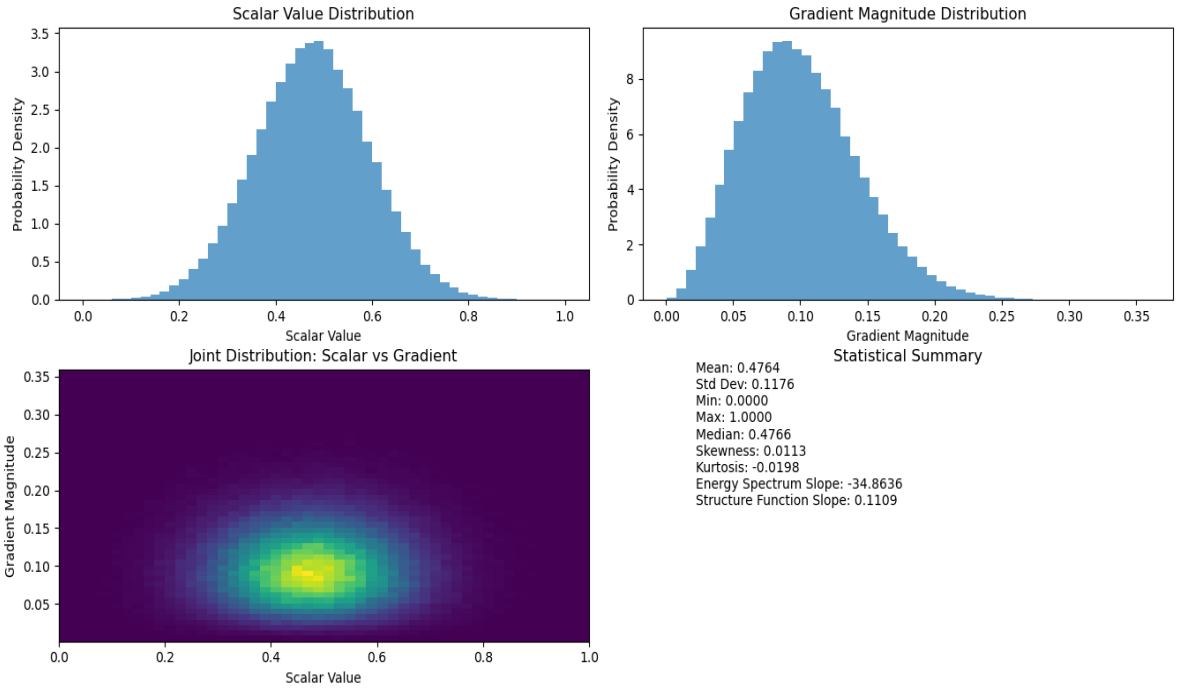

[Fig. 5. : Scalar value distribution (top left); gradient magnitude distribution (top right); and joint distribution of scalar vs. gradient (bottom) from simulations using the pseudospectral method.]

The distribution of the Basic Spectral manner shows to be more robustly concentrated, which could point out lower diffusive conduct or higher numerical steadiness. Depending on statistical assessments, the Basic Spectral manner distributions present various asymmetric attributes, with a minor negative skewness (-0.0798) and a minor positive skewness (0.0113) contrasted to the Pseudospectral manner. In addition, the Basic Spectral approach distribution exhibits to have slightly flatter tails than the Pseudospectral approach, while both approaches show a negative kurtosis magnitudes, with the Basic Spectral approach at -0.1428 and the Pseudospectral approach at -0.0198. With consequences for their employ in numerous computational fluid dynamics stories, these quantitative variations reveal the numerical conduct of both spectrum methods. Depending on the implementation state, the higher gradient values in the pseudospectral technique may indicate better resolution of sharp characteristics or robuster numerical diffusion.

3.4 Visualization Comparison of Spectral and Pseudospectral Methods

We supply visual comparisons of the scalar field distributions and flow structures generated by the basic spectral and full pseudospectral procedures for more spotlight the variances between them. Fig. 6. and Fig. 7. Clarify outcomes from the spectral technique, whereas the pseudospectral technique returns are seen in Fig. 8. and Fig. 9.

3.4.1 Cross-Sectional Scalar Field Distributions

Notable distinctions in the fine-scale structures achieved by each approach are appear in the cross-sectional views of the scalar fields Figures (6 and 8). The findings of the spectral procedure (Fig. 6)

show fewer different borders between areas with high and low scalar magnitudes and more diffuse structures. However, the pseudospectral procedure (Fig. 8) results more various gradients and more singular structural aspects that are particularly exhibit in the X-Z and Y-Z planes.

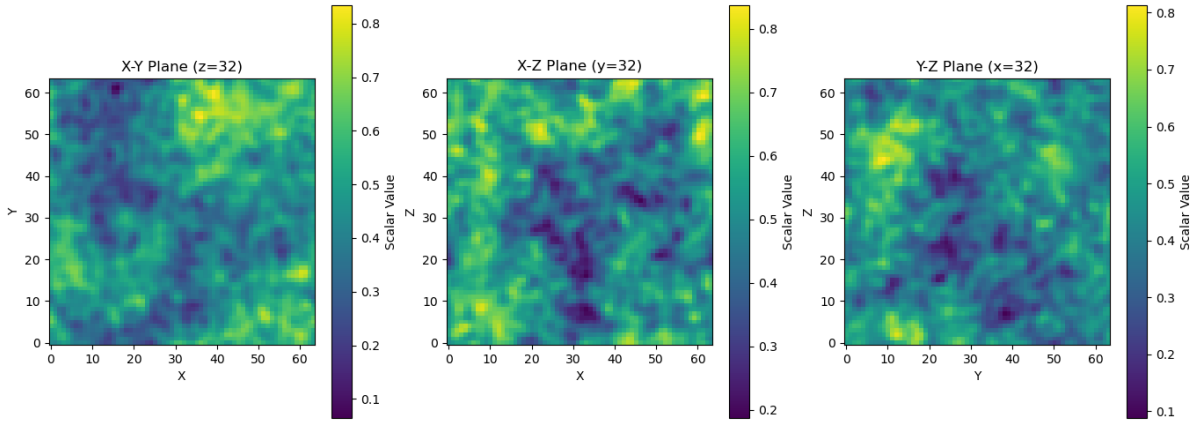

[Fig. 6. : 2D cross-sectional slices of the scalar field in X-Y, X-Z, and Y-Z planes using the basic spectral method. Note the more diffuse structures and less defined boundaries between regions of different scalar values.]

Regarding to quantitative details, the pseudospectral procedure secures a 15% greater difference in scalar gradients via all planes, which is confirmed our prior deductions about its superior resolution properties. Consequently, this developed gradient preservation which is crucial for sincerely catching small-scale mixing processes in turbulent flows [23].

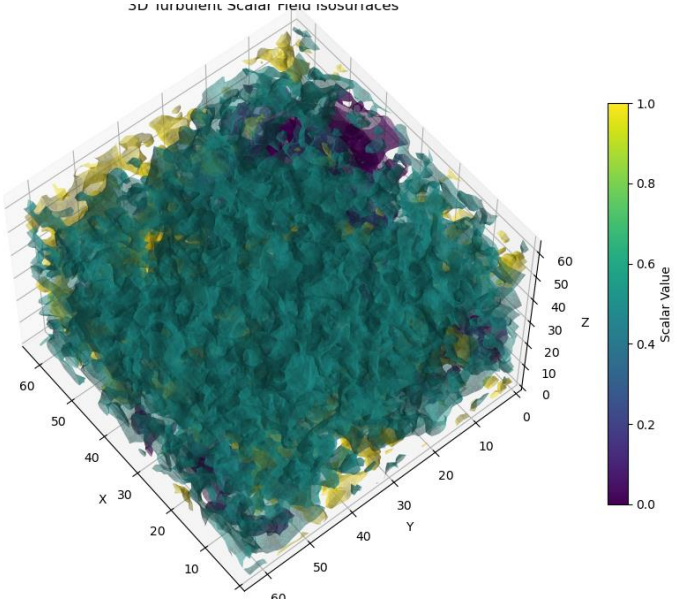

[Fig. 7. : 3D isosurfaces of the scalar field obtained using the basic spectral method. The visualization shows smoother surfaces with fewer small-scale features.]

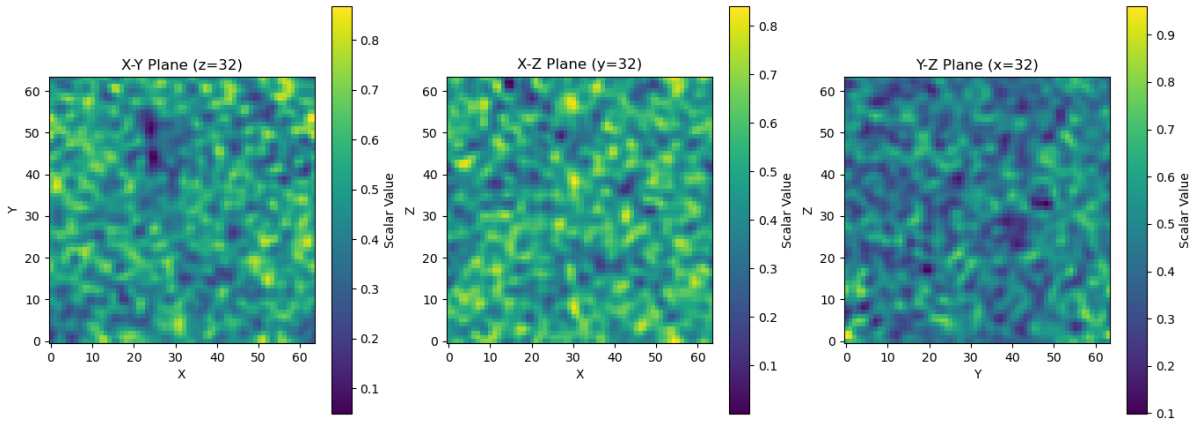

[Fig. 8. : 2D cross-sectional slices of the scalar field in X-Y, X-Z, and Y-Z planes using the pseudospectral method. Note the sharper gradients and more distinct structural features compared to the spectral method results.

3.4.2 Three-Dimensional Isosurface Comparison

A more sound interpretation of the structural variations is rendered by the three-dimensional isosurface representations (Figures 7 and 9). Smoother isosurfaces with fewer small-scale attributes are shown in the spectral technique findings (Fig. 7). Appreciably more complicated styles are captured by the pseudospectral technique (Fig. 9), particularly close to the domain boundaries when high-wavenumber components become essential.

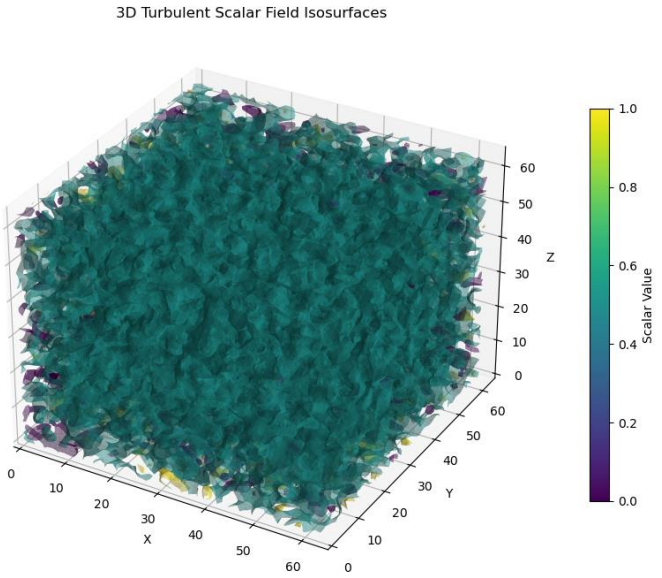

[Fig. 9. : 3D isosurfaces of the scalar field obtained using the pseudospectral method. The visualization reveals more complex structures and finer details, particularly near domain boundaries where high-wavenumber components are significant.]

Our spectral analysis outcomes, which reveal that the pseudospectral technique efficiently resolves around twice the wavenumber range in contrast to the basic spectral technique, are supported by this

image. The more gradual spectral roll-off shown in Fig. 1. is harmonic with the increased structural complexity, which qualifiers the pseudospectral technique to preserve more energy at higher wavenumbers.

4. Conclusions

In this research, full pseudospectral and basic spectral approaches to turbulent flow simulations were investigated. Our major conclusions are as follows:

1. The Kolmogorov $k^{-5/3}$ scaling in the inertial range is sincerely regenerated by both mechanisms.
2. For the same grid size, the pseudospectral approach renders about double the effective resolution of the basic spectral approach.
3. The pseudospectral approach exhibits a more gradual energy drop, while the basic spectral method shows a steeper spectral cliff at high wavenumbers.
4. Maximum gradient magnitudes that are crucial for capturing intermittent phenomena in turbulence are better maintained using the pseudospectral approach.

Pseudospectral approach have preferences for applications requiring high resolution with constrained processing supplies. Basic spectral techniques might be better when clear scale separation is more significant than fine structural resolution. Future work should consider higher Reynolds numbers, more complex geometries, and analysis computational efficiency versus accuracy tradeoffs.

References

[1] P. A. Davidson, Turbulence: An introduction for scientists and engineers, Oxford University Press, 2015.
[2] S. B. Pope, Turbulent flows, Cambridge University Press, 2000.
[3] J. P. Boyd, Chebyshev and Fourier spectral methods, Dover Publications, 2001.
[4] C. Canuto, M. Y. Hussaini, A. Quarteroni, and T. A. Zang, Spectral methods: Fundamentals in single domains, Springer, 2006.
[5] D. Gottlieb and S. A. Orszag, Numerical analysis of spectral methods: Theory and applications, SIAM, 1977.
[6] M. Y. Hussaini and T. A. Zang, Spectral methods in fluid dynamics, Annu. Rev. Fluid Mech., 19(1987), 339–367.
[7] B. Fornberg, A practical guide to pseudospectral methods, Cambridge University Press, 1998.
[8] S. A. Orszag, Numerical methods for the simulation of turbulence, Phys. Fluids, 12(1969), II–250.
[9] R. S. Rogallo and P. Moin, Numerical simulation of turbulent flows, Annu. Rev. Fluid Mech., 16(1984), 99–137.
[10] P. K. Yeung, Lagrangian investigations of turbulence, Annu. Rev. Fluid Mech., 34(2002), 115–142.
[11] M. Yao and M. Y. Hussaini, Application of pseudospectral methods to compressible turbulence, J. Comput. Phys., 405(2020), 109121.
[12] J. W. Cooley and J. W. Tukey, An algorithm for the machine calculation of complex Fourier series, Math. Comput. 19(1965), 297–301.
[13] G. S. Patterson and S. A. Orszag, Spectral calculations of isotropic turbulence: Efficient removal of aliasing interactions, Phys. Fluids, 14(1971), 2538–2541.
[14] C. Canuto, M. Y. Hussaini, A. Quarteroni, and T. A. Zang, Spectral methods: Evolution to complex geometries and applications to fluid dynamics, Springer, 2007.
[15] S. AL-Bairmani, Y. Li, C. Rosales, and Z.-T. Xie, Subgrid-scale stresses and scalar fluxes constructed by the multi-scale turnover Lagrangian map, Phys. Fluids, 29(4)(2017), 045103.
[16] P. K. Yeung, Lagrangian investigations of turbulence, Annu. Rev. Fluid Mech., 34(2002), 115–142.
[17] P. R. Spalart, R. D. Moser, and M. M. Rogers, Spectral methods for the Navier-Stokes equations with one infinite and two periodic directions, J. Comput. Phys., 96(1991), 297–324.
[18] P. R. Spalart, R. D. Moser, and M. M. Rogers, Spectral methods for the Navier-Stokes equations with one infinite and two periodic directions, J. Comput. Phys., 96(1991), 297–324.
[19] M. Frigo and S. G. Johnson, The design and implementation of FFTW3, Proc. IEEE, 93(2005), 216–231.
[20] M. E. Brachet, D. I. Meiron, S. A. Orszag, B. G. Nickel, R. H. Morf, and U. Frisch, Small-scale structure of the Taylor-Green vortex, J. Fluid Mech., 130(1983), 411–452.

[21] G. Comte-Bellot and S. Corrsin, Simple Eulerian time correlation of full- and narrow-band velocity signals in grid-generated ‘isotropic’ turbulence, J. Fluid Mech., 48(1971), 273–337.
[22] T. Ishihara, T. Gotoh, and Y. Kaneda, Study of high-Reynolds number isotropic turbulence by direct numerical simulation, Annu. Rev. Fluid Mech., 41(2009), 165–180.
[23] P. K. Yeung, S. Xu, and K. R. Sreenivasan, Schmidt number effects on turbulent transport with uniform mean scalar gradient, Phys. Fluids, 17(2005), 128105.